

Slow-light enhancement of radiation pressure in an omnidirectional-reflector waveguide

M. L. Povinelli,^{a)} Mihai Ibanescu, Steven G. Johnson, and J. D. Joannopoulos

Department of Physics and the Center for Materials Science and Engineering, Massachusetts Institute of Technology, 77 Massachusetts Avenue, Cambridge, Massachusetts 02139

(Received 23 January 2004; accepted 6 July 2004)

We study the radiation pressure on the surface of a waveguide formed by omnidirectionally reflecting mirrors. In the absence of losses, the pressure goes to infinity as the distance between the mirrors is reduced to the cutoff separation of the waveguide mode. This divergence at constant power input is due to the reduction of the modal group velocity to zero, which results in the magnification of the electromagnetic field. Our structure suggests a promising alternative, microscale system for observing the variety of classical and quantum-optical effects associated with radiation pressure in Fabry–Perot cavities. © 2004 American Institute of Physics. [DOI: 10.1063/1.1786660]

The group velocity of light can be dramatically slowed in photonic crystals. Slow light enhances a variety of optical phenomena, including nonlinear effects, phase-shift sensitivity,¹ and low-threshold laser action due to distributed feedback gain enhancement.^{2,3} Here, we demonstrate that slow light can also enhance radiation pressure. Using numerical calculations, we show how a slow-light, photonic-crystal structure incorporating omnidirectionally reflecting mirrors can be used to maximize the radiation pressure between two surfaces.

For Fabry–Perot cavities, the effect of radiation pressure on the motion of the mirror surfaces has been extensively studied. The magnification of field intensity inside the cavity results in strong optomechanical coupling, leading to interesting classical effects such as optical bistability⁴ and quantum optical effects such as the generation of nonclassical states of light^{5,6} and the potential entanglement of macroscopic objects through optomechanical cooling.⁷ In the Fabry–Perot system, the direction of light propagation is fixed perpendicular to the mirror surfaces, and the reflectivity of at least one mirror is necessarily less than one to allow light to couple into the cavity. We introduce a generalized system that lifts both restrictions and is particularly well suited for embodiment in microscale devices.

The *omnidirectional-reflector waveguide* structure we consider is formed by two omnidirectional mirrors⁸ separated by a distance comparable to the wavelength. Light travelling in the waveguide gives rise to a radiation pressure between the mirror surfaces that depends on the intensity and the mode characteristics. We first optimize the mirror structure to maximize the radiation pressure for fixed electromagnetic energy in the field. We then calculate the radiation pressure as a function of distance as the mirrors are pushed together. As the distance decreases, intensity buildup results from the reduction of the group velocity of the waveguide mode. We show that in the absence of losses, the force *diverges* at waveguide cutoff for constant input power.

The system is shown in Fig. 1(a). Two semi-infinite multilayer films are separated by an air region of thickness d . Each of the films consists of a stack of alternating high- and

low-dielectric layers with period a . For definiteness, we take the refractive indices to be $n_{\text{hi}}=3.45$ and $n_{\text{lo}}=1.45$, corresponding to Si and SiO₂ at 1.55 μm . The relative layer thicknesses are determined by the quarter-wave condition $n_{\text{hi}}d_{\text{hi}}=n_{\text{lo}}d_{\text{lo}}$, which we later show to be an optimal case, along with the constraint that $d_{\text{hi}}+d_{\text{lo}}=a$, yielding $d_{\text{hi}}=0.296a$ and $d_{\text{lo}}=0.704a$. Waveguide modes can be supported in the air region between the films. Superimposed on Fig. 1 is the fundamental guided mode, propagating in the direction shown.

It is sufficient to consider solutions of Maxwell's equations that are uniform in the y direction. The electric field can then be written in the form $\mathbf{E}(x, y, z, t) = \text{Re}[\mathbf{E}_{k, \omega}(z)e^{ikx - i\omega t}]$, where we have made use of the translational symmetry in the x direction. The solutions can be divided into transverse electric (TE) modes ($\mathbf{E} \parallel \hat{y}$ and $\mathbf{H} \perp \hat{y}$), and transverse magnetic (TM) modes ($\mathbf{H} \parallel \hat{y}$ and $\mathbf{E} \perp \hat{y}$). The TE dispersion relation is shown in Fig. 1(b), where the dimensionless quantity $\omega a / 2\pi c$ is plotted as a function of $ka / 2\pi$. Modes were computed by plane-wave expansion.⁹ Shown in grey are the modes of an infinite multilayer film system, or bulk modes. Colored symbols indicate the dispersion relation for the fundamental waveguide mode for several values of d/a . A frequency and wave vector within the band gap of the bulk system indicates that the mode is guided in the air region between the films. For each value of d/a , the group velocity of the guided mode goes to zero at $ka / 2\pi = 0$. As a/d decreases, the mode shifts down in frequency, and higher-order modes will enter the band gap. We focus on the force on the multilayer films produced by light travelling in the fundamental guided mode.

The force was calculated using a Maxwell stress-tensor formalism.^{10,11} The time-averaged force is given by

$$F_{\alpha} = \oint_S da \sum_{\beta} \frac{1}{8\pi} \text{Re} \left[\epsilon E_{\alpha}^* E_{\beta} - \frac{1}{2} \delta_{\alpha\beta} \epsilon |E|^2 + \mu H_{\alpha}^* H_{\beta} - \frac{1}{2} \delta_{\alpha\beta} \mu |H|^2 \right] n_{\beta}, \quad (1)$$

where the integral is taken over a surface S enclosing a volume V , which we take to be a box with parallel faces of area A at $z=0$ and $z=Z$; \hat{n} is the outward surface normal. For guided modes, the contribution from the face at Z goes to zero as $Z \rightarrow \infty$. The contribution from the sides of the box is

^{a)}Electronic mail: mpovinel@alum.mit.edu

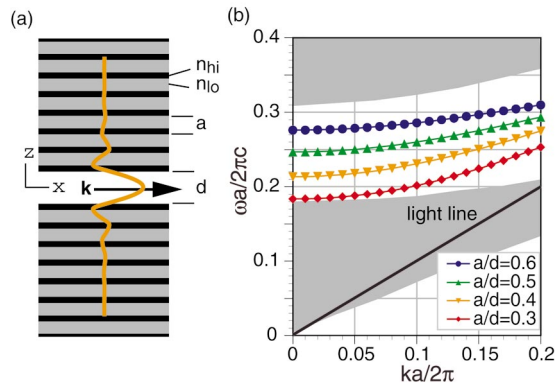


FIG. 1. (Color) (a) Omnidirectional-reflector waveguide structure: Two multilayer films of period a are separated by a distance d ; each film is composed of alternating layers with refractive indices n_{hi} and n_{lo} . Guided modes propagate in the air region between the films in the direction indicated by the wave vector \mathbf{k} . The field profile of the fundamental mode is superimposed on the figure. (b) Dispersion relation for the structure shown in (a) for modes with $\mathbf{E} \parallel \hat{y}$. The high- and low-index layer thicknesses were taken to satisfy the quarter-wave condition for $n_{hi}=3.45$ and $n_{lo}=1.45$. Shaded grey regions indicate bulk modes of the multilayer film, and colored symbols indicate the dispersion relation for the fundamental mode of the waveguide for several different values of a/d .

also zero, since terms from parallel faces cancel, and the total force is given by the midplane integral. It can be easily seen that F_x and F_y are identically zero; as a result of the mirror symmetry of the structure with respect to the $z=0$ plane, modes can always be chosen such that either $\{E_z, H_x, H_y\}$ or $\{H_z, E_x, E_y\}$ is zero there. The time-averaged force per area A in the z direction on the upper film reduces to

$$F/A = -\frac{1}{16\pi} \text{Re}(E_z^* E_z - E_x^* E_x - E_y^* E_y + H_z^* H_z - H_x^* H_x - H_y^* H_y). \quad (2)$$

To determine the optimal multilayer structure, we first consider the maximum achievable optical force for a fixed separation between the multilayer films and a fixed amount of energy in the electromagnetic field (as contrasted to fixed input power). The electromagnetic fields at a given frequency were calculated using planewave expansion.⁹ Figure 2(a) illustrates the dependence of the force on the frequency ω and the period a . We plot the dimensionless quantity Fd/U_{field} as a function of $\omega a/2\pi c$ for several values of a/d , where F is the force due to area A , and U_{field} is equal to the integral of the electromagnetic energy density over A and z . The value of Fd/U_{field} is always positive: The effect of the light in the guided mode is to push the two films apart. For each value of a/d , the force increases with decreasing frequency until it reaches the cutoff frequency of the mode, $\omega(k=0)$ [see also Fig. 1(a)]. We note that the maximum value of the force F_{max} is independent of polarization, since TE and TM modes are degenerate at $k=0$.

It can be shown by either quantum mechanical or classical arguments¹² that, for a dielectric or metallic structure characterized by parameter shift ξ , supporting a single mode at frequency ω and wave vector \mathbf{k} , the time-averaged force on the dielectric is given by

$$F = -\frac{1}{\omega} \frac{\partial \omega}{\partial \xi} \bigg|_{\mathbf{k}} U_{\text{field}}, \quad (3)$$

where it is assumed that the modal field decays to zero perpendicular to the propagation direction. It can be seen from

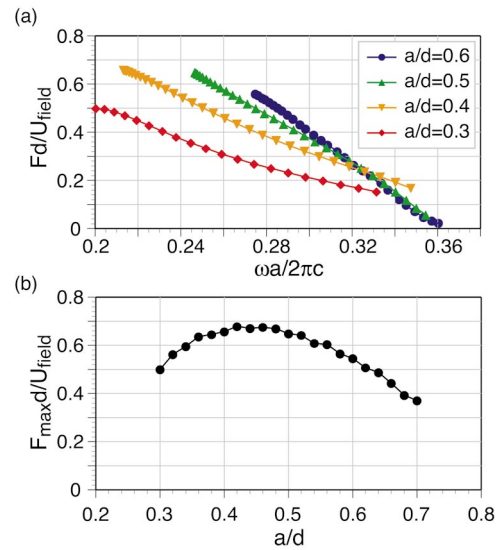


FIG. 2. (Color) (a) Force between the multilayer films resulting from light travelling through the waveguide. Plotted is the dimensionless quantity Fd/U_{field} as a function of the dimensionless quantity $\omega a/2\pi c$, where F is the force due to area A , U_{field} is the electromagnetic field energy contained in a slice of the waveguide that intersects the z axis in area A , and ω is the waveguide mode frequency. (b) Maximum force from (a) as a function of a/d . The peak in the curve gives the maximum attainable force for fixed separation of the films d and energy in the fields U_{field} , where the maximization is over the period of the films a and the frequency ω .

Fig. 1(b) that for a given pair of multilayer films (fixed a), the frequency of the guided mode at a fixed wave vector changes most quickly with displacement d at $k=0$ (i.e., the lines labeled by a/d are furthest apart at $k=0$), consistent with Fig. 2(a).

In Fig. 2(b), we plot $F_{\text{max}}d/U_{\text{field}}$ as a function of a/d . The value increases and then decreases with a/d , peaking near $a/d=0.45$. Referring to Fig. 1(b), we see that the largest force is obtained for values of a/d for which the frequency of the waveguide mode at $k=0$ is near the center of the band gap. In this range, the confinement of the electromagnetic field to the air region between the films is highest, and the values of the electromagnetic fields on the midplane are maximized, leading to the largest force; $F \approx 0.68U_{\text{field}}/d$. For similar reasons, the quarter-wave stack is an optimal structure: Choosing the relative layer thicknesses to satisfy the quarter-wave condition maximizes the $k=0$ band gap, allowing the greatest modal confinement and hence the largest force. We have verified this statement explicitly by fixing $a/d=0.45$ and varying d_{hi} and d_{lo} .

We next consider the distance dependence of the force. Suppose we choose the operating frequency ω and the period a so as to maximize the force at distance d_o for fixed electromagnetic field energy U_{field} . That is, we choose $a=0.45d_o$ and $\omega=\omega(k=0, a/d_o=0.45)$. As the separation is decreased from some initial value to d_o , the force increases, as shown in Fig. 3(a). The group velocity of the waveguide mode at ω simultaneously decreases to zero.

Now consider what happens at fixed input power, a more relevant constraint for any experimental realization of such a device. The energy in the field can be written as $U_{\text{field}} = P_{\text{in}}L/v_g$, where L is the length in the propagation direction of the volume V with cross-sectional area A . In Fig. 3(b), we plot the dimensionless quantity $f(d/d_o) \equiv Fd_o/P_{\text{in}}(L/c)$. As can be seen from the graph, $f \rightarrow \infty$ as $d/d_o \rightarrow 1$. At fixed

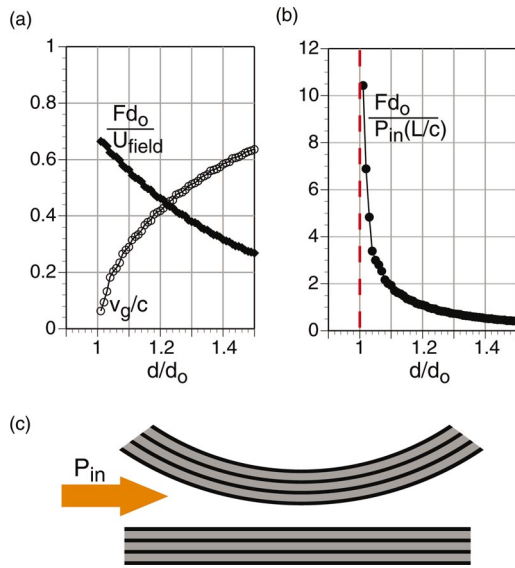


FIG. 3. (Color) (a) Force as a function of separation between the films, for fixed operating frequency and electromagnetic field energy. As d is decreased to d_o , the group velocity of the waveguide mode decreases to zero, shown as the dimensionless quantity v_g/c . (b) Force as a function of separation between the plates, for fixed operating frequency and waveguide input power. As d is decreased to d_o , the force goes to infinity. (c) A possible geometry for achieving constant input power over a range of separations.

frequency and input power, the force between the films is given by

$$F(d) = f(d/d_o) \frac{P_{in}(L/c)}{d_o}, \quad (4)$$

and the force becomes infinite as the separation between the plates approaches d_o . Physically, as the distance between the plates decreases, the group velocity of the waveguide mode decreases to zero. For a fixed power input, the light takes longer and longer to travel down the waveguide, and the magnitude of the field builds up, leading to a divergence in the force. For separations smaller than d_o , the operating frequency is below the cutoff frequency of the mode, and the fields will decay evanescently along the waveguide, reducing the force.

In practice, the divergence at d_o will be removed by loss mechanisms, including losses due to finite mirror thickness, material absorption, input coupling, and scattering from disorder. An accurate numerical estimate of the achievable force will thus depend on a detailed analysis of these mechanisms.

Figure 3(c) shows one means of achieving a nearly constant power input for a range of separations. Here, a cylinder coated with a multilayer film forms the top surface of the waveguide. This geometry not only eases the alignment requirements between the two surfaces, but also forms an adiabatic input taper for coupling, e.g., a tightly focussed laser mode, to the guided mode of the waveguide. Due to the taper, a change in the minimum film separation will correspond to a much smaller fractional change in the film separation at the input, yielding a nearly constant input power. Moreover, any reflections from the output taper back into the waveguide will in fact increase the total force, as they increase the total amount of power in the waveguide.

For larger separations between the multilayer films, the central air waveguide will be multimode. The total force between the films is given by the sum over the force contribu-

tions due to the individual modes. As a result, the force as a function of distance will exhibit peaks at the cutoff distances of each of the higher-order modes. Unlike the case of radiation pressure in mirrored Fabry–Perot cavities,⁴ these peaks are assymmetric around the cutoff length.

Since the key condition for a force divergence is a zero-group-velocity mode at nonzero frequency, a divergence is also expected for metallic waveguides. In the absence of loss, the time-averaged force on the metallic waveguide walls is calculated to be

$$\frac{Fd}{P_{in}(L/c)} = \frac{\pi nc}{2\omega} \frac{1}{\sqrt{d^2 - \left(\frac{\pi nc}{\omega}\right)^2}},$$

for either TE or TM modes. ($F=0$ for the transverse electromagnetic mode, since its frequency is independent of waveguide width.) The force at constant input power thus diverges as $d \rightarrow \pi nc/\omega$ and the mode reaches cut off. However, to maximize the force, the distance between the plates (and consequently the operating wavelength) should be made as small as possible. Due to the high losses in metals at optical wavelengths, the force divergence should be far easier to observe in dielectric systems.

A number of applications of this work should follow from the ability to modify the mechanical oscillation of the structure by optical means, such as sensitive control and positioning on the microscale. A related effect may also occur for radiation pressure on particles.¹³ Operating our structure in reverse, by using an applied force to modify the waveguide group velocity, results in a tunable time-delay device. Moreover, since our omnidirectional-reflector waveguide may be viewed as a Fabry–Perot cavity operated via a sidewise-coupling scheme, it should provide an interesting alternate system in which to explore the rich collection of classical and quantum effects resulting from strong optomechanical coupling in Fabry–Perot systems.

One of the authors (M.L.P.) thanks J. B. Pendry, F. Capasso, N. Mavalvala, D. Kielpinski, D. Iannuzzi, M. Troccoli, and Chiyun Luo for useful discussions. This work was funded in part by the MRSEC program of the NSF under Award No. DMR-9400334.

¹M. Soljačić, S. G. Johnson, S. Fan, M. Ibanescu, E. Ippen, and J. D. Joannopoulos, *J. Opt. Soc. Am. B* **19**, 2052 (2002).

²J. P. Dowling, M. Scalora, M. J. Bloemer, and C. M. Bowden, *J. Appl. Phys.* **75**, 1896 (1994).

³L. Florescu, K. Busch, and S. John, *J. Opt. Soc. Am. B* **19**, 2215 (2002), and references therein.

⁴P. Meystre, E. M. Wright, J. D. McCullen, and E. Vignes, *J. Opt. Soc. Am. B* **2**, 1830 (1985).

⁵C. Fabre, M. Pinard, S. Bourzeix, A. Heidmann, E. Giacobino, and S. Reynaud, *Phys. Rev. A* **49**, 1337 (1994).

⁶S. Mancini, V. I. Man'ko, and P. Tombesi, *Phys. Rev. A* **55**, 3042 (1997).

⁷D. Vitali, S. Mancini, L. Ribichini, and P. Tombesi, *J. Opt. Soc. Am. B* **20**, 1054 (2003), and references therein.

⁸Y. Fink, J. N. Winn, S. Fan, C. Chen, J. Michel, J. D. Joannopoulos, and E. L. Thomas, *Science* **282**, 1679 (1998).

⁹S. G. Johnson and J. D. Joannopoulos, *Opt. Express* **8**, 173 (2001).

¹⁰J. D. Jackson, *Classical Electrodynamics*, 3rd ed. (Wiley, New York, 1998), Sect. 6.7.

¹¹M. I. Antonoyiannakis and J. B. Pendry, *Phys. Rev. B* **60**, 2363 (1999).

¹²M. L. Povinelli, S. G. Johnson, and J. D. Joannopoulos (unpublished).

¹³R. Gómez-Medina, P. San José, A. García-Martín, M. Lester, M. Nieto-Vesperinas, and J. J. Sáenz, *Phys. Rev. Lett.* **86**, 4275 (2001).